

High Strain Rate Superplasticity in a Micro-grained Al–Mg–Sc Alloy with Predominant High Angle Grain Boundaries

F.C. Liu^{1,2)}, Z.Y. Ma^{1)†} and F.C. Zhang²⁾

1) Shenyang National Laboratory for Materials Science, Institute of Metal Research, Chinese Academy of Sciences, Shenyang 110016, China

2) State Key Laboratory of Metastable Materials Science and Technology, Yanshan University, Qinhuangdao 066004, China

[Manuscript received September 19, 2011, in revised form November 16, 2011]

Friction stir processing (FSP) was applied to extruded Al–Mg–Sc alloy to produce fine-grained microstructure with a grain size of 2.2 μm . Electron backscatter diffraction (EBSD) result showed that the grain boundary misorientation distribution was very close to a random grain assembly for randomly oriented cubes. Superplastic investigations in the temperature range of 425–500 °C and strain rate range of 1×10^{-2} – 1×10^0 s^{-1} showed that a maximum elongation of 1500% was achieved at 475 °C and a high strain rate of 1×10^{-1} s^{-1} . The FSP Al–Mg–Sc exhibited enhanced superplastic deformation kinetics compared to that predicted by the constitutive relationship for superplasticity in fine-grained aluminum alloys. The origin for enhanced superplastic deformation kinetics in the FSP alloy can be attributed to its high fraction of high angle grain boundaries (HAGBs). The analyses of the superplastic data and scanning electron microscopy (SEM) examinations on the surfaces of deformed specimens indicated that grain boundary sliding is the main superplastic deformation mechanism for the FSP Al–Mg–Sc alloy.

KEY WORDS: Superplasticity; Friction stir processing; Aluminum; Microstructure; Friction stir welding

1. Introduction

The development of highly formable Al–Mg based alloys is of great interest to the automotive industry, because they provide a lightweight alternative to steel sheet structural panels^[1]. In order to achieve high elongation in these alloys, significant efforts have been made to refine the grain size of these alloys. Chauhan *et al.*^[2] produced ultrafine-grained (UFG) 5083Al (grain size ~ 440 nm) by gas atomization, cryomilling, and consolidation. This alloy exhibited elongations of more than 300% at strain rates of higher than 1×10^{-1} s^{-1} ^[2]. Equal channel angular pressed (ECAP) 5083Al with a grain size of 0.3 μm showed a maximum elongation of 315% at 275 °C and 5×10^{-4} s^{-1} ^[3]. A low-temperature rolled

5083Al exhibited an elongation of 511% at 230 °C and 2×10^{-3} s^{-1} ^[4]. Superplasticity of fine-grained 5083Al alloy is limited primarily by significant grain growth during superplastic deformation.

By comparison, commercial 5083Al modified by adding trace amounts of Sc or Zr as a microstructural stabilizer exhibited a maximum elongation of 740% at 500 °C and 1×10^{-2} s^{-1} ^[5]. Furthermore, a maximum elongation of 1150% was obtained at 570 °C and 2×10^{-3} s^{-1} in a 0.2% Zr and 1.6% Mn modified 5083Al alloy^[6]. It demonstrated that the addition of Sc or Zr improved formability of 5083Al alloy significantly.

Recently, a series of Al–Mg–Sc alloys were developed as highly-formable aluminum alloys with superior properties (especially yield strength) compared to conventional Al–Mg alloys with the same magnesium content^[7]. The well-distributed coherent Al_3Sc precipitates in the alloys are thermodynamically stable

† Corresponding author. Prof., Ph.D.; Tel./Fax: +86 24 83978908; E-mail address: zym@imr.ac.cn (Z.Y. Ma).

and very effective in stabilizing the microstructure^[8]. Previous studies showed that ultrafine-grained Al–Mg–Sc alloys with a grain size of 0.2–1 μm remained very stable even at temperatures higher than 450 $^{\circ}\text{C}$, and very high elongations could be achieved in these alloys at the high temperature and high strain rate ranges^[9–11].

Friction stir processing (FSP), a new metal-working technique^[12,13], caused intense plastic deformation and elevated temperature in the stir zone (SZ), resulting in the generation of fine recrystallized grains of 0.1–12 μm with predominant high-angle grain boundaries (HAGBs) of 85%–97%^[12–17]. This percentage is significantly higher than that in conventional thermo-mechanically treated (TMT) aluminum alloys with a typical HAGB percentage of 50%–65%^[18,19] and in multi-pass ECAP aluminum alloys with a percentage of $\sim 70\%$ ^[20]. High percentage of HAGBs is beneficial to grain boundary sliding (GBS) during superplastic deformation. However, the mobility of HAGBs is high^[21]. The high fraction of HAGBs in the FSP aluminum alloys would affect its thermal stability adversely. Previous studies showed that UFG FSP aluminum alloys exhibited excellent low-temperature superplasticity due to its high percentage of HAGBs^[22–24]. Furthermore, high strain rate superplasticity (HSRS) with high elongations was also achieved in many FSP aluminum alloys at high temperatures. The grains in these alloys were extremely stable due to the pinning of high density of fine particles^[25–27].

In a recent report, we achieved an exceptionally high HSRS in a FSP Al–Mg–Sc alloy with grain size of 2.6 μm ^[27]. However, detailed microstructural examinations, especially on the grain boundary characteristics, and deformation mechanism analyses on the FSP fine grained Al–Mg–Sc alloy are lacking. In the present study, an Al–5.3Mg–0.23Sc alloy was subjected to FSP at a low heat input of 400 r/min and 25 mm/min and superplastic investigation. The aim of the present study is to elucidate the correlation of operative superplastic deformation mechanism and grain boundary characteristics.

2. Experimental

An extruded Al–Mg–Sc plate with chemical composition of Al–5.33Mg–0.23Sc–0.49Mn–0.14Fe–0.06Zr (wt%) was used as raw material. A single-pass FSP was carried out at a tool rotation rate of 400 r/min and a traverse speed of 25 mm/min, using a steel tool with a concave shoulder of 14 mm in diameter and a threaded conical pin of 5 mm in root diameter and 3.5 mm in tip diameter, and 4.5 mm in length.

Microstructural characterization was performed on the cross-section of the stir zone (SZ) transverse to the FSP direction by scanning electron microscopy (SEM). The samples for SEM were lightly electropolished to produce a strain-free surface. Elec-

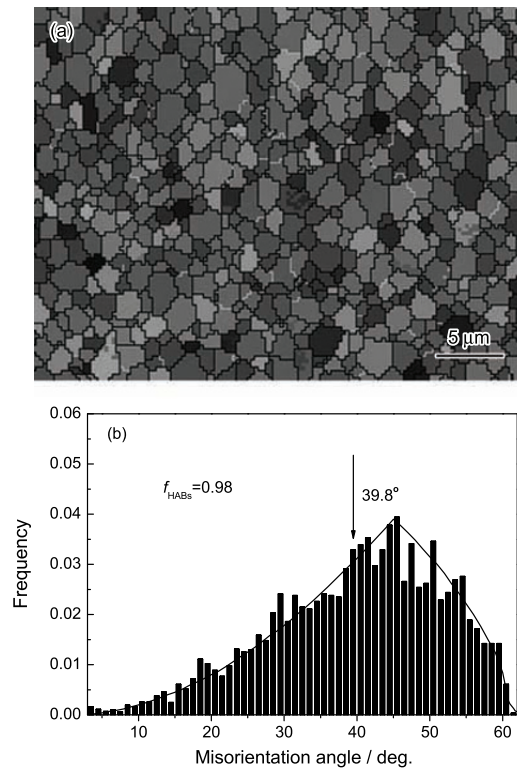


Fig. 1 Microstructure of FSP Al–Mg–Sc alloy: (a) EBSD map, (b) boundary misorientation angle distribution

tron backscatter diffraction (EBSD) orientation maps (with a resolution of 80 nm) were obtained by using a ZEISS SUPRA 35, operated at 20 kV, and interfaced to an HKL Channel EBSD system.

Dog-bone shaped superplastic tensile specimens (2.5 mm in gage length, 1.4 mm in gage width and 1.0 mm in gage thickness) were electro-discharge machined from the SZ of the FSP sample transverse to the FSP direction. These specimens were subsequently ground and polished to a final thickness of ~ 0.8 mm. Tensile tests with a constant crosshead speed were conducted by using an INSTRON 5848 micro-tester. Each specimen was held at the testing temperature for about 15 min in order to reach thermal equilibrium. The failed specimens were subjected to SEM examinations.

3. Results

Fig. 1(a) shows the microstructure of the FSP Al–Mg–Sc sample obtained by EBSD mapping, in which the black and white lines represent the high angle grain boundaries (HAGBs, grain boundary misorientation angle $>15^{\circ}$) and low angle grain boundaries (LAGBs, grain boundary misorientation angle $<15^{\circ}$), respectively. FSP resulted in the generation of the fully recrystallized microstructure with a uniform and equiaxed grain distribution, and the average grain size was determined to be 2.2 μm . The misorientation angle histogram of the FSP Al–Mg–Sc sample is shown in Fig. 1(b). This misorientation distribution is very

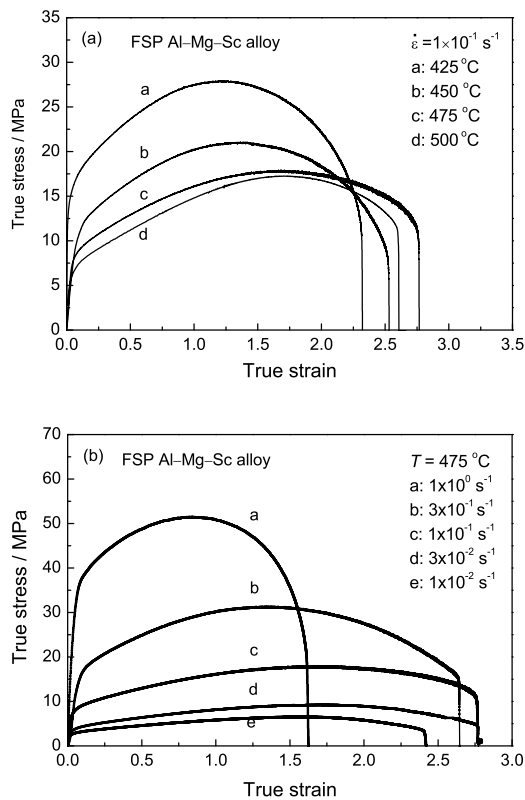


Fig. 2 Effect of (a) temperature and (b) strain rate on true stress-true strain curves for FSP Al-Mg-Sc alloy

close to a random grain assembly predicted by Mackenzie for randomly oriented cubes^[28]. The number fraction of HAGBs was 98%, which is very close to 97% for a true random grain assembly^[28]. The average misorientation angle was determined to be 39.8° and very close to 40.7° for a random misorientation distribution predicted by Mackenzie^[28].

Fig. 2 shows the typical true stress-true strain curves for the FSP Al-Mg-Sc sample at an initial strain rate of $1 \times 10^{-1} \text{ s}^{-1}$ for different temperatures ranging from 425 to 500 °C (Fig. 2(a)) and at 475 °C for different initial strain rates ranging from $1 \times 10^{-2} \text{ s}^{-1}$ to 1 s^{-1} (Fig. 2(b)). No obvious steady-state flow region was observed. Extensive strain hardening took place initially. After reaching a maximum, the flow stress continuously decreased until failure. Increasing temperature led to a shift of the peak stress to a higher strain. A similar phenomenon was found in ECAP 1570Al alloy deformed at $1.4 \times 10^{-2} \text{ s}^{-1}$ ^[6] and TMP 5083 Al deformed at $2.8 \times 10^{-3} \text{ s}^{-1}$ ^[18].

Fig. 3(a) shows the variation of elongation with initial strain rate for the FSP Al-Mg-Sc sample. At 425 °C, a maximum elongation of 1250% was achieved at a high strain rate of $3 \times 10^{-2} \text{ s}^{-1}$. With increasing the temperatures to 450–500 °C, the largest ductility was achieved at higher strain rates of 3×10^{-2} – $1 \times 10^{-1} \text{ s}^{-1}$. At 475 °C, a maximum elongation of 1500% was observed at the strain rates of 3×10^{-2} –

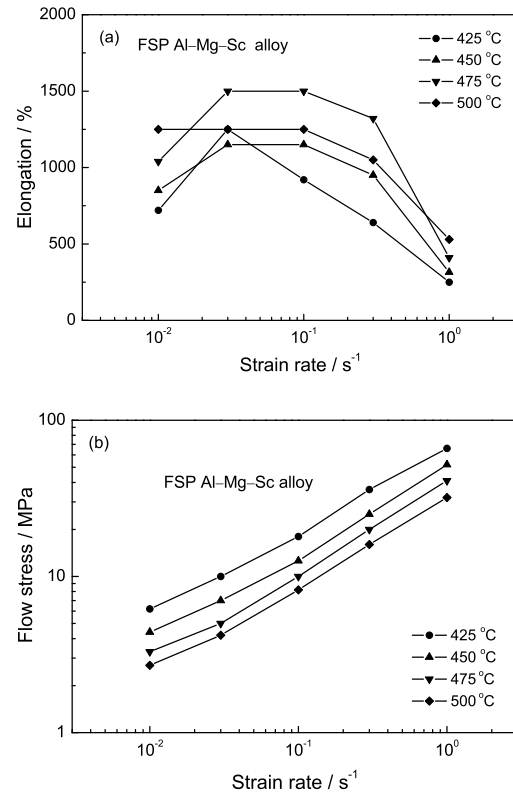


Fig. 3 Variation of (a) elongation and (b) flow stress with initial strain rate for FSP Al-Mg-Sc alloy

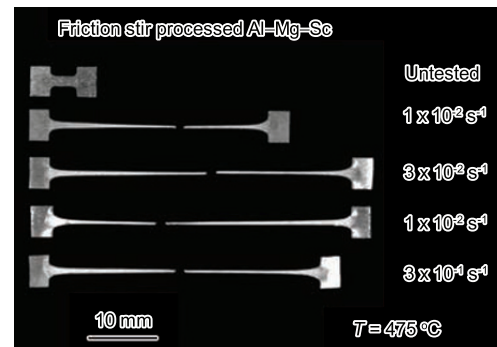


Fig. 4 Specimens of FSP Al-Mg-Sc alloys tested at 475 °C and various strain rates

$1 \times 10^{-1} \text{ s}^{-1}$. Elongations of $\geq 1000\%$ were obtained in a wide temperature range of 425–500 °C.

Fig. 3(b) shows the variation of flow stress (at true strain of 0.1) with initial strain rate for the FSP sample. The strain rate sensitivity m of the FSP sample was ~ 0.5 in the strain rates of 1×10^{-2} – 1 s^{-1} at the investigated temperature range. The specimens showed relatively uniform elongation characteristic of superplastic flow (Fig. 4).

To reveal the superplastic deformation mechanism of the FSP Al-Mg-Sc sample, the surfaces of tensile specimens deformed at $1 \times 10^{-1} \text{ s}^{-1}$ and various temperatures to elongation of 900% were subjected to SEM examinations. GBS was distinctly observed on the surfaces of the deformed specimens (Fig. 5). All

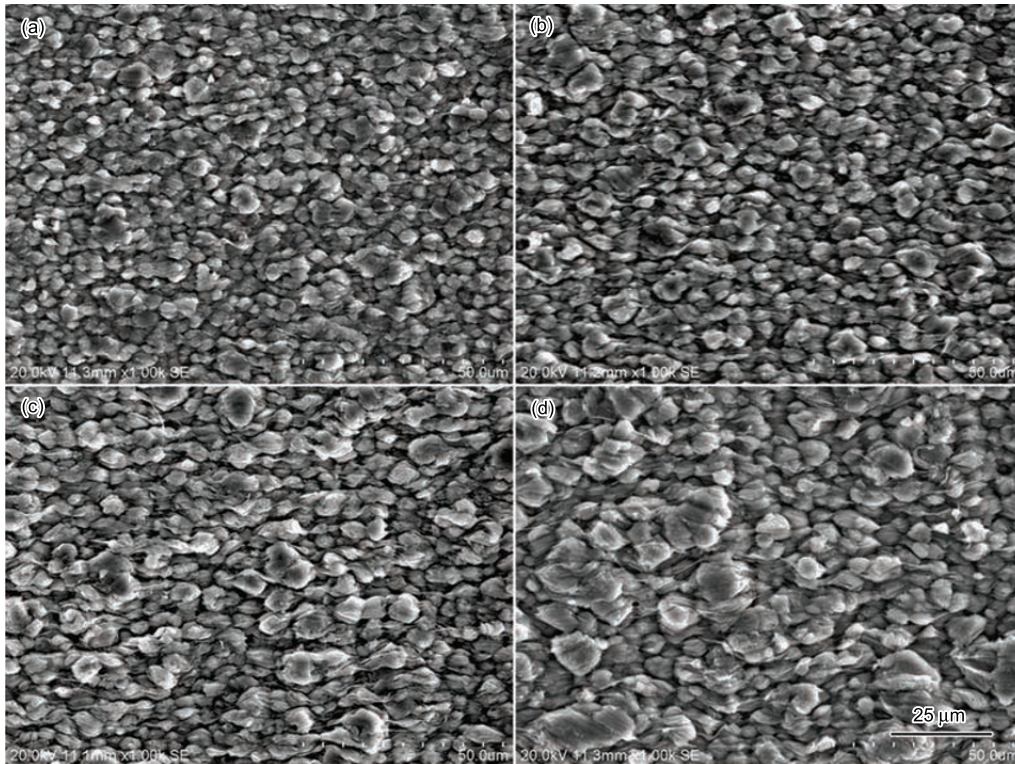


Fig. 5 SEM micrographs showing surface topographies of failed tensile specimens deformed to 900% at $1 \times 10^{-1} \text{ s}^{-1}$ and various temperatures: (a) 425 °C, (b) 450 °C, (c) 475 °C and (d) 500 °C

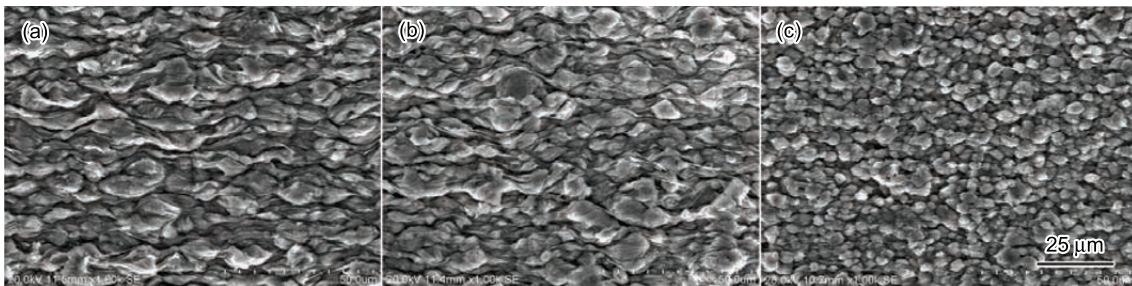


Fig. 6 SEM micrographs showing surface topographies of failed tensile specimens deformed to 900% at 475 °C and various strain rates: (a) $1 \times 10^{-2} \text{ s}^{-1}$, (b) $3 \times 10^{-2} \text{ s}^{-1}$ and (c) $3 \times 10^{-1} \text{ s}^{-1}$

the specimens deformed at $1 \times 10^{-1} \text{ s}^{-1}$ exhibited equiaxed grain morphology at various temperatures. This topography was similar to that of FSP 7075Al deformed at 480 °C and $1 \times 10^{-1} \text{ s}^{-1}$ which was characterized by extensive GBS and equiaxed grains^[13]. The FSP Al–Mg–Sc exhibited higher elongation than FSP 7075Al under similar deformation conditions due to finer grain size of the FSP Al–Mg–Sc and its better thermal stability at high temperature. Increasing the temperature from 425 to 475 °C did not result in a distinct increase in the grain size. This also indicates that the fine-grained structure of the FSP Al–Mg–Sc was relatively stable during high temperature deformation. At a higher temperature of 500 °C, it appears that the size of the grains increased significantly. This is consistent with the superplastic result that the maximum elongation decreased significantly

at 500 °C.

Fig. 6 shows the topography of the specimens deformed to failure at 475 °C and various strain rates. At strain rates of 1×10^{-2} – $3 \times 10^{-2} \text{ s}^{-1}$, extensive GBS along with somewhat elongated grains was observed. When the strain rate was increased to $3 \times 10^{-1} \text{ s}^{-1}$, GBS and equiaxed grains were distinctly observed on the surface of the deformed specimen. Furthermore, decreasing the strain rate resulted in the increase of the grain size, which is attributed to the increased time for high-temperature exposure.

4. Discussion

It is well documented that friction stir welding (FSW)/FSP generates significant frictional heating and intense plastic deformation, thereby creating fine and equiaxed recrystallized grains in the SZ^[22–27,29].

Typical grain sizes observed in the FSW/FSP aluminum alloys are in the order of micrometer. However, Rhodes *et al.*^[30] obtained recrystallized grains of 25–100 nm in FSP 7050Al-T76 by using “plunge and extract” technique and rapid cooling. When heated at 350–450 °C for 1–4 min, these grains grew to 2–5 μm, a size equivalent to that found in the FSP aluminum alloys^[30].

Considering the existence of a high density of fine Al₃Sc particles dispersed throughout the matrix in the present Al–Mg–Sc alloy, a fine grain-sized (2.2 μm) Al–Mg–Sc was obtained after FSP because the grain growth during FSP was significantly retarded by the high Zener pinning^[20]. Previous study showed that an even finer grain sized (0.6 μm) Al–Mg–Sc was produced by FSP with water cooling^[16]. These demonstrate that the micro-sized grains in the FSP Al–Mg–Sc were developed from the nano-sized newly-recrystallized grains at elevated temperature during FSP. The dynamic grain growth during FSP resulted in a misorientation distribution in the FSP Al–Mg–Sc which is very close to a random grain assembly predicted by Mackenzie for randomly oriented cubes^[28].

It is generally accepted that grain boundary sliding (GBS) is the dominant deformation mechanism during superplastic flow for most of fine-grained materials when the strain rate sensitivity of flow stress is approximately 0.5. The microstructural prerequisites for GBS are an excellent combination of stable equiaxed fine-grained structure and dominant HAGBs. However, the aluminum alloys produced by rolling or extrusion usually exhibited an unrecrystallized microstructure characterized by a high ratio of LAGBs. LAGBs are generally believed to be not suitable for GBS owing to their low orientation differences^[31]. This unrecrystallized microstructure gradually evolved into a structure consisting of new recrystallized grains with increasing the strain. Approximately equiaxed grain structure with a high fraction of HAGBs appeared at high strains. However, the transformation of LAGBs to HAGBs usually resulted in a significant grain growth, which reduced the deformation rate and/or superplastic elongation.

The present FSP Al–Mg–Sc was characterized by fine recrystallized grains with a high fraction of HAGBs. Such a microstructure is a typical structure facilitating the occurrence of GBS in the initial superplastic stage. Furthermore, the grain growth at high temperatures in the FSP Al–Mg–Sc is slow due to the presence of fine Al₃Sc particles both at the grain boundaries and within the grain interiors^[16]. Therefore, it is not surprising that a maximum elongation of 1500% was achieved at high strain rates of 3×10^{-2} – $1 \times 10^{-1} \text{ s}^{-1}$ and 475 °C.

The constitutive relationship for superplasticity in fine-grained aluminum alloys can be expressed as^[32],

$$\dot{\epsilon} = 40 \frac{D_0 E b}{k T} \exp\left(\frac{-84000}{RT}\right) \left(\frac{b}{d}\right)^2 \left(\frac{\sigma - \sigma_0}{E}\right)^2 \quad (1)$$

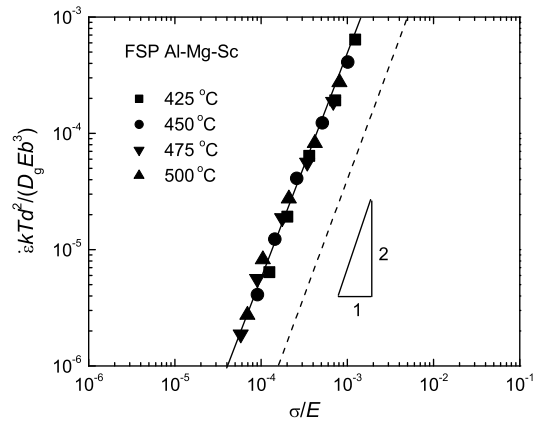


Fig. 7 Variation of $\dot{\epsilon} k T d^2 / (D_g E b^3)$ with normalized stress for FSP Al–Mg–Sc alloy

where $\dot{\epsilon}$ is the strain rate, D_0 is the pre-exponential constant for diffusivity, E is Young’s modulus, b is Burger’s vector, k is Boltzmann’s constant, T is the absolute temperature, R is the gas constant, d is the grain size, σ is the applied stress, and σ_0 is the threshold stress.

To further elucidate the superplastic deformation mechanism in the FSP Al–Mg–Sc sample, superplastic data are plotted in Fig. 7 as $(\dot{\epsilon} k T d^2 / (D_g E b^3))$ vs σ / E . For comparison, a dashed line predicted by Eq. (1) is also included in Fig. 7. Three important observations can be made from this plot. First, the temperature dependence of superplastic flow for the FSP Al–Mg–Sc is similar to the activation energy for aluminum grain boundary self-diffusion. Second, the data of the FSP sample fit into a single straight line with a slope of 2, showing that the stress dependence of superplastic flow is approximately 2 ($\dot{\epsilon} \propto \sigma^2$). Third, a dimensionless constant that fit the data for the FSP sample was larger than 40 found in Eq. (1). A stress exponent of 2 and an activation energy close to that for grain boundary self-diffusion are associated with the GBS models of Mukherjee^[33] and Ball and Hutchinson^[34]. Thus, Fig. 7 shows that GBS is the main superplastic deformation mechanism for the FSP Al–Mg–Sc sample.

In this analysis, superplastic data of the FSP Al–Mg–Sc sample can be described by

$$\dot{\epsilon} = 620 \frac{D_0 E b}{k T} \exp\left(\frac{-84000}{RT}\right) \left(\frac{b}{d}\right)^2 \left(\frac{\sigma}{E}\right)^2 \quad (2)$$

The dimensionless constant of 620 in Eq. (2) is larger than 40 in Eq. (1). Ma *et al.*^[26] examined the superplastic data of FSP 7075Al rolled plates with two different grain sizes of 3.8 and 7.5 μm, and a dimensionless constant of 790 was observed by normalizing the superplastic data. Similarly, Johannes and Mishra^[35] obtained a much higher constant of 1396 in a FSP 7075Al with a grain size of 4.7 μm. The higher dimensionless constants than 40 (Eq. (1)) imply that the flow stresses of the FSP alloys were lower

than that predicted by Eq. (1) at a given temperature, grain size, and strain rate. This is attributed to higher percentage of the HAGBs in the FSP alloys that facilitate the GBS during the superplastic deformation.

The overall implication of the present results is quite significant. These results show the effectiveness of using a simple FSP technique to produce fine-grained microstructure with predominant HAGBs which exhibited excellent superplasticity at strain rates as high as 10^{-1} s^{-1} in the Al–Mg–Sc alloy under low stress. The analyses of the superplastic data indicate that GBS is the main deformation mechanism with a higher dimensionless constant than that in the traditional constitutive relationship. The enhanced superplastic properties and deformation kinetics in the FSP Al–Mg–Sc were attributed to its high fraction of HAGBs.

5. Conclusions

(1) 2.2 μm grain-sized Al–Mg–Sc alloy with the misorientation distribution very close to a random grain assembly for randomly oriented cubes was produced by friction stir processing.

(2) FSP Al–Mg–Sc exhibited superplastic elongations of >1000% in a wide temperature range of 450–500°C and high strain rate range of 3×10^{-2} – $3 \times 10^{-1} \text{ s}^{-1}$. A maximum elongation of 1500% was achieved at 475°C and a high strain rate of $1 \times 10^{-1} \text{ s}^{-1}$.

(3) SEM examinations on the surface of deformed specimens revealed distinct evidence of extensive GBS. Both dynamic grain growth and grain elongation along the tensile axis were observed in the specimens deformed at lower strain rates while the specimens deformed at higher strain rates exhibited equiaxed grain morphology at various temperatures.

(4) The analyses of the superplastic data indicate that GBS is the main deformation mechanism with a dimensionless constant of 620, a stress exponent of 2 and an activation energy close to that for grain boundary self-diffusion. The enhanced superplastic deformation kinetics in the FSP Al–Mg–Sc was attributed to its high fraction of high angle grain boundaries.

Acknowledgements

The authors gratefully acknowledge the support of the National Natural Science Foundation of China under Grant Nos. 50671103 and 50871111 and the National Outstanding Young Scientist Foundation of China under Grant Nos. 50525103 and 50925522.

REFERENCES

- [1] T.G. Nieh, L.M. Hsiung, J. Wadsworth and R. Kaibyshev: *Acta Mater.*, 1998, **46**, 2789.
 [2] M. Chauhan, I. Roy and F.A. Mohamed: *Metall. Mater. Trans. A*, 2006, **37**, 2715.
 [3] K. Taepark, D.Y. Hwang, S.Y. Chang and D.H. Shin: *Metall. Mater. Trans. A*, 2002, **33**, 2859.
 [4] I.C. Hsiao and J.C. Huang: *Metall. Mater. Trans. A*, 2002, **33**, 1373.
 [5] K.T. Park, D.Y. Hwang, Y.K. Lee, Y.K. Kim and D.H. Shin: *Mater. Sci. Eng. A*, 2003, **341**, 273.
 [6] R. Kaibyshev, F. Musin, D.R. Lesuer and T.G. Nieh: *Mater. Sci. Eng. A*, 2003, **342**, 169.
 [7] Y.A. Filatov, V.I. Yelagin and V.V. Zakharov: *Mater. Sci. Eng. A*, 2000, **280**, 97.
 [8] K.L. Kendig and D.B. Miracle: *Acta Mater.*, 2002, **50**, 4165.
 [9] Z. Horita, M. Furukawa, M. Nemoto, A.J. Barnes and T.G. Langdon: *Acta Mater.*, 2000, **48**, 3633.
 [10] F. Musin, R. Kaibyshev, Y. Motohashi and G. Itoh: *Scripta Mater.*, 2004, **50**, 511.
 [11] R. Kaibyshev, E. Avtokratova, A. Apollonov and R. Davies: *Scripta Mater.*, 2006, **54**, 2119.
 [12] R.S. Mishra and M.W. Mahoney: *Mater. Sci. Forum*, 2001, **357**, 507.
 [13] Z.Y. Ma, R.S. Mishra and M.W. Mahoney: *Acta Mater.*, 2002, **50**, 4419.
 [14] Z.Y. Ma, R.S. Mishra, M.W. Mahoney and R. Grimes: *Mater. Sci. Eng. A*, 2003, **351**, 148.
 [15] I. Charit and R.S. Mishra: *Mater. Sci. Eng. A*, 2003, **359**, 290.
 [16] F.C. Liu, Z.Y. Ma and L.Q. Chen: *Scripta Mater.*, 2009, **60**, 968.
 [17] K.A.A. Hassan, A.F. Norman, D.A. Price and P.B. Prangnell: *Acta Mater.*, 2003, **51**, 1923.
 [18] T.R. McNelley and M.E. McMahon: *Metall. Mater. Trans. A*, 1997, **28**, 1879.
 [19] M. Eddahbi, T.R. McNelley and O.A. Ruano: *Metall. Mater. Trans. A*, 2001, **32**, 1093.
 [20] M. Ferry, N.E. Hamilton and F.J. Humphreys: *Acta Mater.*, 2005, **53**, 1097.
 [21] D. Juul Jensen: *Acta Mater.*, 1995, **43**, 4117.
 [22] F.C. Liu and Z.Y. Ma: *J. Mater. Sci.*, 2009, **44**, 2647.
 [23] F.C. Liu and Z.Y. Ma: *Scripta Mater.*, 2008, **58**, 667.
 [24] Z.Y. Ma and R.S. Mishra: *Scripta Mater.*, 2006, **53**, 75.
 [25] Z.Y. Ma, R.S. Mishra, M.W. Mahoney and R. Grimes: *Metall. Mater. Trans. A*, 2005, **36**, 1447.
 [26] Z.Y. Ma, R.S. Mishra, and M.W. Mahoney: *Acta Mater.*, 2002, **50**, 4419.
 [27] F.C. Liu and Z.Y. Ma: *Scripta Mater.*, 2008, **59**, 882.
 [28] J.K. Mackenzie: *Biometrika*, 1958, **45**, 229.
 [29] R.S. Mishra and Z.Y. Ma: *Mater. Sci. Eng. R*, 2005, **50**, 1.
 [30] C.G. Rhodes, M.W. Mahoney, W.H. Bingel and M. Calabrese: *Scripta Mater.*, 2003, **48**, 1451.
 [31] P.S. Bate, N. Ridley and B. Zhang: *Acta Mater.*, 2007, **55**, 4995.
 [32] R.S. Mishra, T.R. Bieler and A.K. Mukherjee: *Acta Metall. Mater.*, 1995, **43**, 877.
 [33] A. Arieli and A.K. Mukherjee: *Mater. Sci. Eng.*, 1980, **45**, 61.
 [34] A. Ball and M.W. Hutchinson: *Metal. Sci. J.*, 1969, **3**, 1.
 [35] L.B. Johannes and R.S. Mishra: *Mater. Sci. Eng. A*, 2007, **464**, 255.